TÜBİTAK

Turkish Journal of Botany

http://journals.tubitak.gov.tr/botany/

Research Article

Turk J Bot
(2022) 46: 92-108
© TÜBİTAK
doi:10.3906/bot-2108-31

In silico analysis of *XTH* gene family from barley (*Hordeum vulgare* L.) and their comparative expression analysis during germination

Hülya AKDEMİR[1], Merve SEVEN[2], Ü. Cem DERMAN[2], Andrew J. HARVEY[2,*]

[1]Gebze Technical University, Department of Molecular Biology and Genetics, Kocaeli, Turkey
[2]Yeditepe University, Department of Genetics and Bioengineering, 34755, İstanbul, Turkey

Received: 16.08.2021 • **Accepted/Published Online:** 29.11.2021 • **Final Version:** 29.03.2022

Abstract: Changes in plant cell walls are critical for expansion and growth. Xyloglucan endotransglycosylase/hydrolase (XTH) enzymes are the major modifiers of xyloglucan within the cell wall and are present as large gene families. Despite the paucity of xyloglucan in barley, our analyses of the barley genome revealed at least 42 *XTH* genes, the most *XTH* members recorded for a monocot genome to date. In this paper, we show a detailed look at the barley *XTH* gene family, including detailed bioinformatics analyses of conserved protein motifs and structure, phylogenetic relationships, and a comparison of the expression patterns during germination and seedling growth using RT-qPCR and RNA-Seq analyses. Overall, there was a good correlation between RT-qPCR and RNA-Seq data for similar tissues. RNA-Seq data showed many different expression profile patterns, from broad, high level expression for some *XTH* genes to highly tissue specific patterns for others. RT-qPCR expression patterns also varied widely between genes. The highest expressing gene, *HvXET4*, had levels around five times that of the highest control gene tubulin. Given the low levels of xyloglucan found in barley, this high level of expression suggests that the enzyme may be catalysing reactions with other cell wall polysaccharides. We propose roles for many of the *HvXTH* genes based on the results shown here.

Key words: Xyloglucan endotransglycosylase/hydrolase, gene family, cell wall modification, phylogenetic analyses, transcript analysis, seedling growth

1.Introduction

Plant cell walls are highly complex and dynamic structures (Vorwerk et al. 2004). The composition and organization of the cell walls of an individual plant vary spatially and temporally according to cell type and the plant's growth stage during cell division, growth, and differentiation (Hematy and Höfte, 2007; Hrmova et al. 2007). Plant cell walls are comprised of cellulose, non-cellulosic polysaccharides, structural proteins, enzymes, lignin and various inorganic molecules (Carpita and McCann, 2000).

Xyloglucan is one of the major non-cellulosic polysaccharides found in the primary cell walls of all higher plants including lycopodiophytes (extant primitive vascular plants), gymnosperms, and angiosperms (Hoffman et al. 2005; Obel et al. 2007). Although it is the most abundant non-cellulosic β-linked polysaccharide in the cell walls of dicots and non-graminaceous monocots (10 to 25% of the dry weight), the graminaceous monocots including the *Poaceae* family contain only 1 to 10% xyloglucan of the dry weight of their primary cell wall (Obel et al. 2007 and references therein). Through strong non-covalent interactions, xyloglucan coats and/or tethers the surface of cellulose microfibrils and it results in providing integrity and direct or indirect regulation of the mechanical properties of the cell wall (McCann et al. 1990; Rose et al. 2002; Zykwinska et al. 2008).

Plant cell growth is achieved by the irreversible expansion of cell walls (Cosgrove 2005; Ivakov and Persson, 2013). All of the analyzed plant genomes show the presence of large gene families encoding cell wall modifying enzymes (Carpita et al. 2001; Mbeguie-A-Mbeguie et al. 2009). Agents such as expansins and xyloglucan endotransglycosylases/hydrolases (XTHs) play critical roles in controlled loosening and, thus, in expansion and growth of the cell wall (Fry et al. 1992; Cosgrove, 2005). The genomes of well-studied plants such as rice and Arabidopsis contain around thirty different *XTH* genes. XTH enzymes are proposed to have important roles in cell wall elongation, since xyloglucan chains are responsible for cross-linking the load-bearing cellulose microfibrils of the cell walls (Takeda et al. 2002). XTH enzymes can have two distinct actions; after endolytically cleaving a xyloglucan

* Correspondence: andrew.harvey@yeditepe.edu.tr

polysaccharide within the cell wall, they can join another xyloglucan polymer or oligosaccharide (xyloglucan endotransglycosylase (XET) activity), or they can join water (xyloglucan endohydrolase (XEH) activity) (Rose et al. 2002). Thus, XET activity can potentially increase chain length, whereas XEH activity always reduces it.

Xyloglucan polysaccharides and oligosaccharides are the preferential substrates of the XTH enzymes reported to date. However, the xyloglucan structure between plants and different cells of a plant can vary greatly. For example, variation in the length and acetylation of xyloglucan subunits was observed in coleoptile samples of barley between days 3 to 6 and alteration in structure was observed (Gibeaut et al. 2005). This alteration may stimulate changes in *XTH* expression patterns, depending on the individual substrate preferences of each enzyme. Thus, knowledge of spatial and temporal expression of the different *HvXTH* genes will be of use in predicting substrate specificities and potential roles of the enzymes.

The amount of xyloglucan in barley is very low, at a maximum of around 10 % of barley coleoptiles cell walls, but it is extremely low or absent in other barley tissues (Sakurai and Masuda 1978; Gibeaut et al. 2005). The barley genome was initially reported to contain at least 22 different *XTH* sequences (Strohmeier et al. 2004; Gibeaut et al. 2005; Hrmova et al. 2007). Two recent papers have reported 24 (Fu et al. 2019) and 36 (Stratilova et al. 2020) *XTH* genes in barley. This current study shows that there are at least 42 *XTH* genes in the barley genome. Such an abundance of genes in a monocot species that theoretically work on xyloglucan, a substrate that is scarce or absent, suggests that the various encoded enzymes may each have highly specific functions within certain cell types or tissues, or even roles in catalysing transfer activities on other polysaccharides. Some xyloglucan endotransglycosylases have been shown to be effective on cell wall polysaccharides other than xyloglucan (Hrmova et al. 2007; Maris et al. 2011), and this might also contribute to a number of different roles for barley (*Hordeum vulgare*) XTH enzymes.

Despite their transferase ability, XTH enzymes are classified by their structure as members of the Glycoside Hydrolase Family 16 (GH16) in the CAZy database (Lombard et al. 2014). When XTH sequences are compared in a phylogenetic tree, several major branches are typically present, including Groups I, II, IIIA, IIIB, and IV (Figure 1; Rose et al. 2002; Yokoyama et al. 2004; Baumann et al. 2007; Seven et al. 2021). More recently, another clade, Endoglucanase 16 (EG16), has been examined, and it appears to contain strict endoglucanases that are likely to represent evolutionary links from a progenitor bacterial gene (Eklöf et al. 2013). Other than the EG16 clade, all other sequences are thought to be transferases, with the exception of Group IIIA, which are predominantly XEH enzymes that can also exhibit some transferase ability (Baumann et al. 2007). Given the supposition that the various clades may indicate groupings of enzymes with different substrate and/or tissue specificities, information on the expression patterns of genes from each clade coupled with knowledge of the cell wall composition of those tissues could be highly valuable.

In this study, we first aimed to investigate the barley *XTH* gene family and analyse how they grouped in a phylogenetic tree. Representatives of each phylogenetic clade could then be studied, by comparing their expression levels in various barley tissues, using both low-throughput (RT-qPCR) and high-throughput (RNA-Seq) methods. This can help our understanding of the roles the different *XTH* genes play in the developmental stages of barley and give wider insight into the variation and potential roles of *XTH* genes in all plants.

2. Materials and methods

2.1 Gene family prediction and phylogenetics

Barley *XTH* gene sequences were identified and retrieved from various public databases (http://webblast.ipk-gatersleben.de/barley_ibsc/; http://barleyflc.dna.affrc.go.jp/bexdb/) using various approaches. The resulting barley XTH protein sequences, together with the rice and Arabidopsis XTHs, as well as PttXET16-34 (AAN17442), the nasturtium predominant-XEH (TmQ07524), and PtEG16 (XP_002301319.1) were included in subsequent phylogenetic analyses (Figure 1, Figure S1a). A *Paenibacillus macerans* Licheninase sequence was included to root the tree (Figure S1b). ClustalX2 (Larkin *et al.*2007) was used to generate multiple sequence alignments (MSA) of the protein sequences (Figure 2, Figure S2) and to create the phylogenetic trees (Figure 1). Phylogenetic trees were visualised using the Dendroscope 3 software (Huson and Scornavacca 2012).

2.2 Bioinformatics analyses of conserved motifs

Highly conserved regions were detected using DREME software (Bailey 2011). Possible signal peptides were analysed using SignalP software (Bendtsen et al.2004) and N-glycosylation patterns were predicted using NetNGlyc (http://www.cbs.dtu.dk/services/NetNGlyc/).

2.3 Primer design for selected barley *XTH* gene products

Primer sets specific to *HvXTH* genes and control genes for RT-qPCR studies were designed depending on *Hordeum vulgare* EST sequences in NCBI database (Table S1). Designed oligonucleotide primers were checked using Premier Biosoft Netprimer software and by BLASTing primer sequences against the NCBI database. Gene specificity of each primer couple was tested by different and independent procedures, including product sequencing and melt curve analysis.

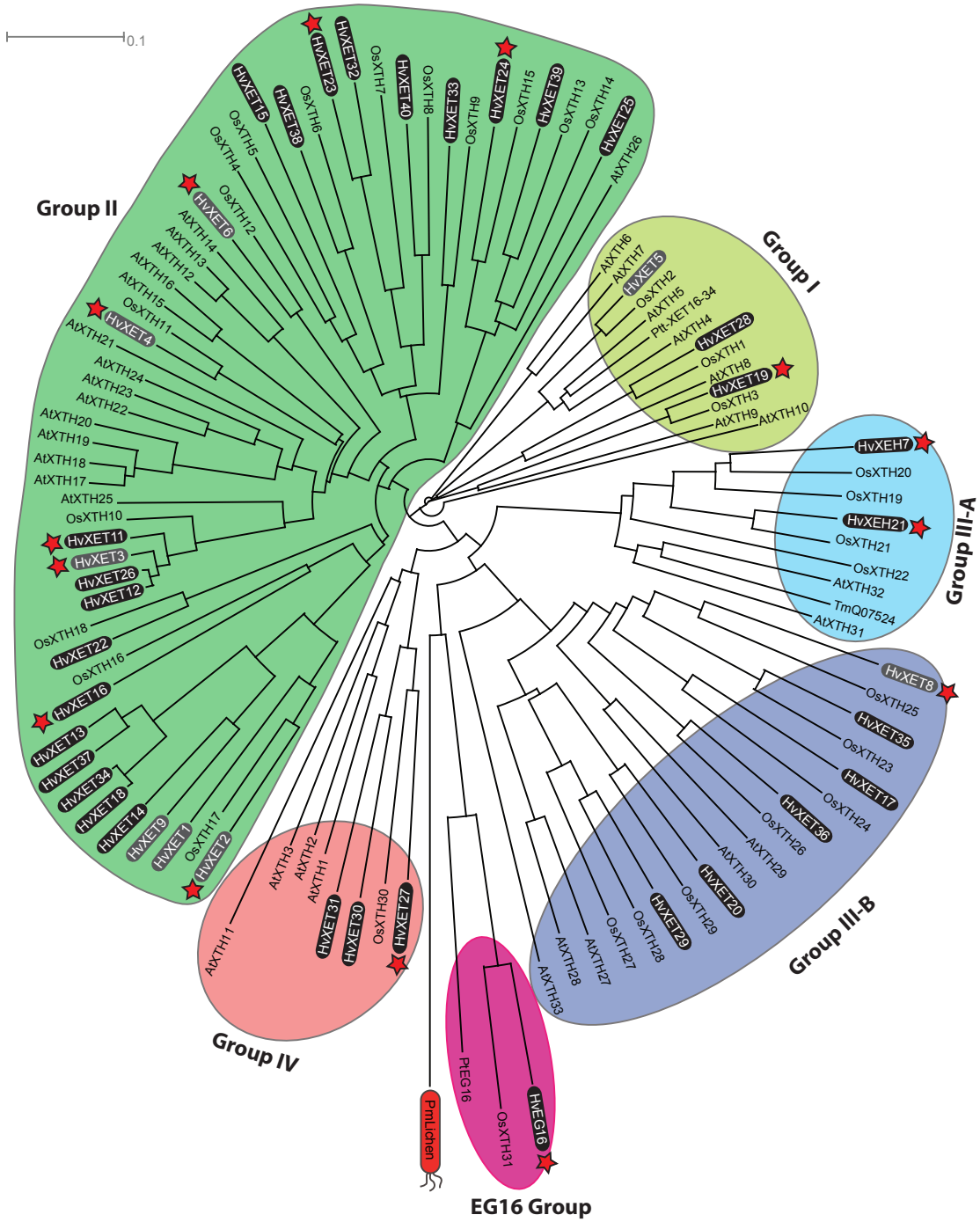

Figure 1. Phylogenetic relationship of barley, rice, Arabidopsis, and selected other XTH proteins. Sequence identifiers can be found in supplemental table 3 (Table S3). Coloured areas indicate the different phylogenetic clades. Red stars indicate the *HvXTHs* whose expression levels were analysed in this study.

2.4 Plant Material

Barley (*Hordeum vulgare* L. cv Zeynelağa) seeds were imbibed in running tap water for 24 hours, and transplanted into Magenta GA-7 vessels containing wet sterile filter paper or into pots with damp perlite, at 22 °C with or without illumination, for germination. Coleoptile samples were collected from dark-kept vessels on day two (CD2), day three (CD3), day four (CD4), day five (CD5) and day six (CD6) for RNA isolation (Table 1). The germinated seeds in the pots were subjected to a 16/8

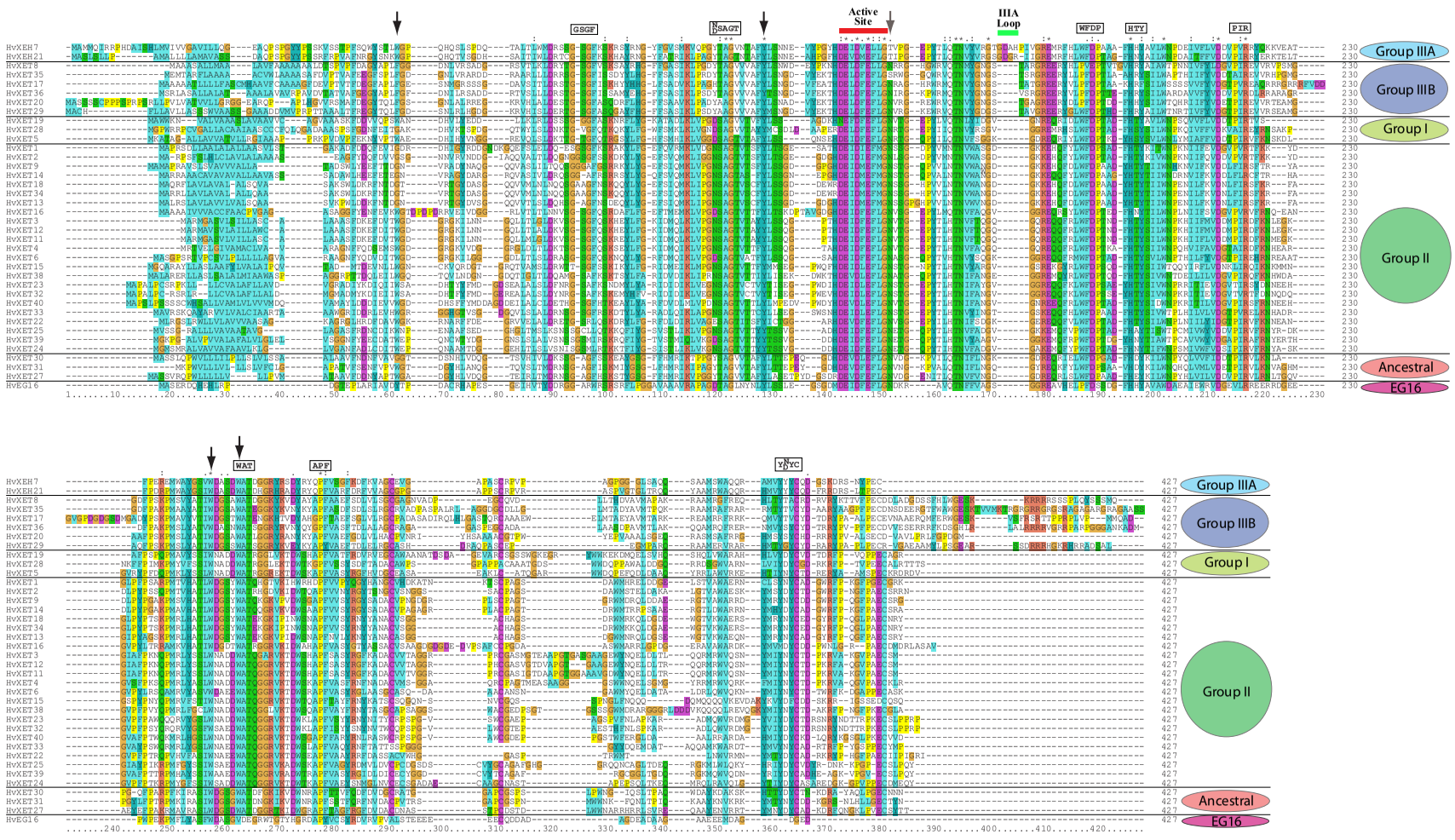

Figure 2. Multiple sequence alignment, using CLUSTAL X2, of all 40 HvXTH protein sequences. Red bar indicates highly conserved active site region. Green bar shows location of Group IIIA loop insertion indicative of XEHs. Grey arrow adjacent to active site region indicates the main potential N-linked glycosylation site. Black arrows indicate the four highly conserved aromatic residues involved in substrate binding. Black text in boxes above the alignment indicate some of the highly-conserved sequences identified by DREME software (see manuscript for details). Coloured ovals on the right of the alignment indicate which sequences group into which phylogenetic clade, as per the phylogenetic tree (see Figure 1).

Table 1. *Hordeum vulgare* cv. Zeynelağa tissue names, abbreviations, sampling times, and cDNA normalization factors.

Plant section	Abbreviation	Sampling time during germination (days)	Normalization Factor
Coleoptile	CD2	2	1.0145
Coleoptile	CD3	3	0.7873
Coleoptile	CD4	4	0.9830
Coleoptile	CD5	5	0.9548
Coleoptile	CD6	6	1.0184
Leaf tip	Leaf A	15	1.0213
Leaf maturation	Leaf B	15	1.0284
Leaf elongation	Leaf C	15	0.9164
Young whole root	Young root	3	0.9078
Root tip	Root A	15	1.1595
Root elongation	Root B	15	1.0632
Root maturation	Root C	15	1.2161

hour light/dark cycle and used for the rest of the sampling (roots and leaves). Young root samples were prepared from 3-days old plant samples. Leaf samples at 15 days old were used for isolation of leaf tip (the top 1 cm of the leaf), leaf elongation region (cell division zone; 1 cm at the base of the leaf) and leaf maturation region (region in between leaf tip and leaf elongation) RNA samples. For root sections, 15-day old roots were used; tip 1 cm of roots were used as root tip donor, 1 cm region closest to stem was used as root maturation region and region in between root tip and root maturation was used as root elongation donor (Table 1). For RNA extraction, 100 mg of each tissue sample was collected from multiple plants. All the collected barley samples were used freshly for RNA extraction.

2.5 RNA extraction and cDNA synthesis

100 mg of each tissue sample was snap-frozen by liquid nitrogen and homogenized using a mortar and pestle. Total RNA extraction from homogenized sample was performed using Easy-spin™ IIp Plant RNA extraction kit (Intron Biotechnology) according to manufacturer's instructions.

Extracted total RNA samples were used for cDNA synthesis with Superscript III first-strand synthesis system (Invitrogen™) using oligo$(dT)_{20}$ as primer according to manufacturer instructions. Synthesized cDNAs were stored at -20 °C.

2.6 Template preparation and HPLC analyses

Stock PCR products of gene specific primers and control gene primers were generated using Pfx50 DNA polymerase (Invitrogen, California). Coleoptile Day 5 (CD5) cDNA was used as template DNA for amplification in a reaction mixture composed of 0.26 µM each of forward and reverse primers, 0.3 mM of dNTP mix, varying amount of $MgSO_4$ depending on the primer couple, 2 µL 10× Pfx50 PCR mix, varying amount of template DNA and 2 units of Pfx50 DNA polymerase. For each primer couple, five independent 20 µL PCR products were combined and quantified and purified by Agilent 1100 HPLC system using an Agilent PLRP-S 1000 Å 5µM 50*2.1 mm reverse-phase column (Burton et al. 2004). HPLC study was performed using buffer A (0.1 M triethylammonium acetate and 0.1 mM EDTA) and buffer B (0.1 M triethylammonium acetate and 0.1 mM EDTA, 25% w/v acetonitrile) with a gradient starting with 63% v/v A, increasing to 74.9% v/v A within 30 minutes, decreasing to 63% v/v A from 30 to 40 min and continuing with 63% v/v A after 40 min at a 0.2 ml/min flow rate. The DNA was detected by A_{260}. Peaks representing 147 bp, 190 bp and 242 bp of pUC19/*Hpa*II digest fragments were used as HPLC standards to quantify the amount of the DNA peak of each PCR product. HPLC purified PCR products were dried and dissolved in nuclease-free water to produce 10^{11} fragments per µL stock solutions.

2.7 RT-qPCR analyses

A dilution series covering 10^7 to 10^2 copies per µL were prepared for control genes and *HvXTH* genes. Dilution series were used as templates in RT-qPCR studies alongside tissue cDNAs. RT-qPCR trials were carried out as three times of two replicates. Each RT-qPCR tube was composed of 1 µL of template DNA, 5 µL of Biorad iTaq Universal SYBR Green Supermix, 4 µM of each primer in a final volume of 10 µL. Reactions were performed as follows: 3 min at 95 °C followed by 40 cycles of 5 s at 95 °C and 30 s at 60 °C on Biorad CFX96 Touch instrument. Melt curve analysis was carried out after each RT-qPCR

amplification by heating the product from 65 °C to 95 °C. The Biorad CFX Manager 3.1 software was used to determine the optimal cycle threshold for experiments. The data acquired was normalized by normalized factors obtained using *HvActin* and *HvTubulin* control genes by GeNorm V3 software. The mean expression level and standard deviation score for each set of six replicates for each cDNA were calculated.

2.8 RNA-Seq analyses

Publicly available data were obtained for RNA-seq experiments performed on barley cultivar Morex at the James Hutton Institute, Dundee, Scotland. The files were downloaded from NCBI from Bioproject PRJEB14349. Raw reads are downloaded as sra files from the Sequence Read Archive and processed to fastq files using SRAtoolkit from NCBI. After initial quality assessment using FastQC, the high quality (phred > 30) reads are aligned to the reference genome using aligners bowtie2 or HiSat (Kim et al. 2015, Langmead et al. 2012). The aligned reads as sequence alignment map (sam) files are further processed (converted into binary alignment (bam) files and sorted) using SAMtools (Li et al. 2009, Li et al. 2011). Further analysis focused on discovered *XTH* genes provided a guide to relevant programs as gtf or bed files. The depth coverage for regions of interest is inspected also with SAMtools as well as visually using genome browsers, e.g., JBrowse (Buels et al. 2016). The expression values as Fragments per Kilobase of transcript per Million mapped reads (FPKM) are calculated using Tuxedo suite, cufflink, and/or cuffdiff programs (Pertea et al. 2016, Trapnell et al. 2010). The differential expression is assessed using high fold change ($|\log2FC| > 2$) and low p-value ($p < 0.01$ from Student's t-test) between control and tissue of interest. Final post processing of the expression values is performed using standard spreadsheet programs.

3. Results

3.1 Bioinformatic analyses of barley *XTHs*

Careful screening of available barley genomic and transcript sequence databases revealed the presence of at least 42 *XTH* genes. All these 42 genes were confirmed as being active genes by having ESTs, FL-cDNA, or other expression data assigned to them. Translated amino acid sequences of all HvXTH proteins were compared in a pairwise fashion and identity and similarity values recorded (Table S2). Identity values varied between a very low 22% up to 98%, whilst similarity ranged between 33%–98%. Genes *HvXET8* and *HvXET14* have identical orthologues in the database and are referred to in supplemental Table S3 as *HvXET8a/HvXET8b* and *HvXET14a/HvXET14b*. Gene *HvXET26* has an identical sequence (*HvXTH26b*; HORVU0Hr1G022110) in the collection of pseudomolecules that have not been assigned to a chromosome (ChrUn), but it is unknown as to whether this is the same gene or a recent gene duplication. Genes *HvXET17* and *HvXET25* also have near-identical orthologues in the genome database (*HvXET17b*; HORVU5Hr1G124040.1 & *HvXET25b*; HORVU2Hr1G110980), but these sequences are incomplete. Whether this is due to the currently incomplete nature of the barley genome sequence, or whether they are pseudogenes is unknown at this time. However, RNA-seq reads still map to these incomplete genes, as shown with the *HvXET25b* data in Table S4, and need to be accounted for.

Two recent papers also studied the *XTH* gene family of barley. Fu and colleagues used BLAST and HMMER searches but were only able to identify 24 *XTH* genes (Fu et al. 2019). A similar approach was taken by Stratilova and colleagues where they limited responses to those containing both the PF00722 (Glyco_hydro_16) and PF06955 (XET_C) known XTH domains and were able to identify 36 *XTH* genes (Stratilova et al. 2020). In this study, we used a variety of search techniques of EST, cDNA, and genomic databases with the active site motif or previously identified plant *XTH* genes and proteins to match against. From this, 42 full length barley *XTH* genes are detected with the possibility of at least a further three being present, including *HvXTH17b*, *HvXTH25b*, and *HvXTH26b*. All 42 have the characteristic highly-conserved catalytic motifs, and comparisons to homologous sequences from other plant XTHs show them to be full-length (Figure S2).

Signal peptides were predicted from the translated protein sequences for 39 of the 40 different sequences. The mature protein sequences ranged in length from 249 to 341 amino acids, varied in MW from 27524 to 37785 Da, and had pIs ranging from 4.01 to 9.18. The impact of such wide variation in isoelectric points is unknown but has been observed before in other XTH families (Atkinson et al. 2009). It should be noted that the average pI for barley XTH enzymes is 6.17, which is much lower than the average pI of 7.89 for Arabidopsis XTHs.

MSAs were created for all translated barley XTH sequences (Figure 2) and for all barley, rice, Arabidopsis, and selected other sequences (Figure S2). A phylogenetic tree (Figure 1) was created using the N-J method in ClustalX2. These analyses revealed that, in the barley *XTH* gene family, there are 3 Group I, 25 Group II, 2 Group IIIA, 6 Group IIIB, 3 Group IV, and 1 EG16 sequence.

All the barley XTH sequences were shown to have the highly conserved DEIDFEFLG active site motif. There is some sequence variation in this motif where amino acids of similar size and charge are substituted, but the catalytic glutamic acids are invariant. The expected loop 2 insertion for Group IIIA XEH enzymes (Baumann et al. 2007) is seen in HvXEH7 and HvXET21 in Figure 2. This is thought to

be associated with conferring the XEH ability (Baumann et al. 2007). Most of the sequences contain 3-4 cysteine residues in the C-terminal region, which are thought to be involved in disulphide bridges that stabilize the helical extension of the C-terminus (Campbell and Bramm 1999; Mark et al. 2009). The Group IIIB sequences of HvXET8, 17, 20, 29, 35, & 36 have a C-terminal extension that is longer than those of the other clades. The function of this extension is unknown and Group IIIB genes, in general, have been poorly studied and warrant further investigation. The sequence for HvXET17, includes a 15-amino acid insertion ~70 residues after the catalytic site. Analysis of the barley genomic sequence shows that there is no intron in this region, and there is a full-length cDNA AK354670 confirming that this gene is expressed with this insertion. Modelling of HvXET17 using 1UMZ (PttXET16-34) as a template revealed this extra sequence to be included as a surface loop, away from the active site and is, thus, unlikely to affect substrate binding or catalysis.

Analyses of the MSAs for conserved regions using DREME software (Bailey 2011), revealed additional motifs with high sequence conservation (Table 2). These motifs, along with four highly conserved Trp residues thought to be involved in substrate binding, were positioned on the MSA (Figure 2). When examining the 3D structure of the poplar XTH, 1UMZ (PttXET16-34), the positions of most of the highly-conserved motifs, other than 'WAT' and the active site motifs, are located away from the substrate binding cleft (Johansson et al. 2004). Thus, it seems likely that motif conservation is more likely involved in overall structural conservation than with substrate recognition. Indeed, we examined the 1UMZ (PttXET16-34) structural model, and the Phe residue in the top hit 'WFDP', present in 106 of the 108 sequences aligned, is positioned ~3.5 Å from the totally conserved His residue of 'HTY', enabling a possible stacking interaction. The Tyr residue of 'HTY', conserved in all but two of the sequences, is ~3.5-4 Å from the Phe of 'GSGF', where it may be able to form a ring-to-edge interaction.

Analysis of the translated barley XTH sequences for potential N-glycosylation sites revealed wide variation in the number and location of predicted glycosylation sites. HvXEH7, 10, 21, 30, & 31 all lacked any detectable glycosylation motifs, whilst other proteins had as many as three predicted sites. The highly-conserved N-glycosylation site found just after the catalytic motif, is present in 28 of the encoded barley XTH proteins, which is a similar ratio to the 21 out of 33 Arabidopsis XTHs with the same motif. It has been shown in heterologous expression experiments that glycosylation is very important for XTH protein stability (Vaaje-Kolstad et al. 2010), thus the lack of any N-glycosylation may indicate that these enzymes have short half-lives and are rapidly turned over. The interpretation of this, especially for HvXEH7 & 21, which are predicted to have predominantly XEH activity, may be important to prevent excess degradation. HvEG16, another potential hydrolase, albeit of the EG16 variety, also lacks any discernible N-glycosylation sites.

Table 2. Highly conserved regions in XTH sequences detected using DREME software (Bailey 2011). The top 10 hits are shown, found from an alignment of all XTHs from barley, rice, and Arabidopsis, as well as poplar XET PttXET16-34, poplar PtEG16, nasturium XEH TmQ07524, and the outgroup bacterial licheninase P23904.2. *Note that the conserved motif 'HTY' becomes almost totally conserved (106/108) when viewed as 'HXY'. Additional abbreviations used: B = Asparagine or Aspartic acid residues, J = Leucine or Isoleucine residues.

Motif	Logo	E-Value	Positives
1	WFDP	4.1e-036	90/108
2	DEJD	1.4e-035	87/108
3	EFLG	1.9e-033	92/108
4	WAT	2.1e-031	103/108
5	YBYC	4.9e-028	79/108
6	BSAGT	2.6e-018	59/108
7	APF	2.6e-016	81/108
8	PIR	5.5e-015	76/108
9	GSGF	1.1e-013	60/108
10	HTY	7.5e-013	56/108*

3.2 RT-qPCR analysis of barley *XTH* expression levels

Initial experimentation showed that creating specific primers for all *HvXTH* genes that would not cross-react with other, highly similar *HvXTH* genes, was not possible. Thus, sequences for RT-qPCR analyses were chosen to represent as broad as possible an examination of the barley XTH gene expression profiles, whilst maintaining total gene specificity. Genes from each of the branches of the phylogenetic tree were included, since it has been postulated that the different clades may represent different substrate specificities/action patterns or modes of activity amongst the XTH enzymes. In particular, HvXET3, HvXET4, and HvXET6 were included since some heterologous expression and substrate specificity data have been published for these sequences (Vaaje-Kolstad et al. 2010, Hrmova et al. 2009, Stratilova et al. 2020). Initially, 30 primer sets were carefully designed and obtained; however, only 15 sets of these gave a product that could be verified as specific for the given gene sequence, as confirmed by melt-curve analyses and repeated DNA sequencing.

The most commonly described roles of XTHs are associated with cell expansion. Coleoptiles, in particular,

represent a model cell elongation system where transcript studies are simplified due to the non-photosynthetic nature of the tissue. Therefore, coleoptile samples were collected from five different stages of coleoptile growth.

All RT-qPCR studies were carried out as at least 6 replicates. Expression levels of various samples and *XTH* genes were normalized using *HvActin* and *HvTubulin* control genes. Normalization factors were acquired using GeNorm (V3) software (Table 1). Normalized c_q values of each gene were used, and mRNA copy number/µL values were calculated through the calibration curves (Table 3).

There is a large variation in transcript numbers of *HvXTH* genes during germination and development of barley plantlets (Figures 3 & 4). *HvXET4* was the gene with highest transcript level during the early development stages, yet there is a huge decrease in their expression levels in the latter days (Figure 3a). At ~196 million transcripts/ul in coleoptile day 2, the expression of *HvXET4* was higher than the highest control gene used, *HvTubulin*. To ensure, the veracity of this result, the sequence of the *HvXET4* PCR product was verified through multiple cloning/sequencing reactions.

HvXET6 transcript number increases during coleoptile growth and expression increases almost ten times between day 5 and day 6 coleoptile samples. In addition, there is relatively high expression in Root Tip, but lower expression in other tissues (Figure 3). *HvXEH7* and *HvXET8* also show a developmental dependent expression in coleoptile tissue. Endoglucanase *EG16* member *HvEG16* showed expression in younger tissues and developing root sections, indicating a possible role of *EG16 XTHs* in earlier development (Figure 3d).

HvXET8 is encoded in the genome by two duplicate genes (HORVU1Hr1G051020, HORVU1Hr1G051040) that are even identical in their promoter regions. It is therefore impossible to distinguish between them using RT-qPCR; however, since their promoter regions are indistinguishable, they are most likely simultaneously transcribed and translated, and their results from the RNA-seq experiments can be additive FPKM values. Likewise, *HvXET14* and *HvXET25* are represented in the barley genome by duplicate genes (HORVU7Hr1G021950 and HORVU7Hr1G021820 for *HvXET14a & b*, HORVU2Hr1G111030 and HORVU2Hr1G111060 for *HvXET25a & b*). A working set of RT-qPCR primers was designed and used for *HvXET14a/b* but the results were incredibly high, most often higher than that of the reference gene α-tubulin. Melt-curve analyses and sequencing of PCR products confirmed the correct product, but on further examination of the barley genome, part of the 3'-untranslated region, which is confirmed by FL-cDNA sequences AK371075 & AK368726, is also present approximately 300,000 bp away on Chr7. At this location the 3'-untranslated region of *HvXET14* is present after an unsequenced region represented by about 40 'N's. Prior to this unsequenced region is a predicted histone H3.2 protein coding region, so if the structure of this portion of the genome is correct, then it is possible that histone gene transcript is adding to the RT-qPCR product. Given that the *HvXET14a* and *HvXET14b* FPKM and

Table 3. Copy numbers of different barley *XTH* mRNAs per µL during germination period of barley plantlets. Representative images of barley plantlets are shown above tissue names on the table. Leaf and root images are placed to correspond to sections they are representing. Table is colour coded to visualize differences of gene expressions between genes and tissues. Red coloured table cells indicate high expression; whereas, as expression gets low, colour firstly turns yellow, then blue. White cells indicate no detected expression.

	CD2	CD3	CD4	CD5	CD6	Leaf A	Leaf B	Leaf C	Young Root	Root A	Root B	Root C
HvXTH2	979,961	222,889	239,474	376,855	334,078	12,234	54,439	60,140	91,134	145,098	18,134	2,796
HvXTH3	3,287,102	486,467	840,591	1,434,882	1,738,164	16,749	62,089	78,393	2,216	625,100	99,250	37,211
HvXTH4	196,237,384	1,020,929	3,311	56,734	7,088	23,874	79,282	6,502	1,343,697	329,335	183,505	1,602,031
HvXTH6	4,235	5,587	29,733	155,785	1,097,890	180,499	199,830	223,366	2,951	703,648	175,864	8,672
HvXTH7	464,552	17,348	700,032	3,429,442	6,164,496	11,340	7,887	2,608	335,230	777,473	722,441	17,177
HvXTH8	116,227	967	5,877	67,441	248,887	629,918	158,432	131,151	74,869	297,085	304,724	238,089
HvXTH10	102,514	286	1,859	1,018	3,133	1,705	541	487	15,114	49,630	58,215	1,802
HvXTH11	1,484,401	73,493	27,991	77,603	95,438	69,413	204,148	20,049	1,571	131,515	71,977	7,108
HvXTH16	660	*Trace*	841	6,198	30,360	2,463,757	770,717	88,993	20,206	217,634	130,761	667,246
HvXTH19	36,711	*Trace*	251	93	523	44	65	73	7,560	58,232	49,090	825
HvXTH21	1,153,014	8,823	1,412	5,642	2,203	336	186	203	11,319	47,154	39,110	1,093
HvXTH23	321	*Trace*	348	99	210	819	1,131	143	16,555	15,382	14,619	2,345
HvXTH24	3,550	*Trace*	2,535	791	2,253	2,511	3,826	153	26,078	214,050	363,536	7,377
HvXTH27	768	*Trace*	207	200	1,276	879	1,179	82	159	21,819	39,806	2,166

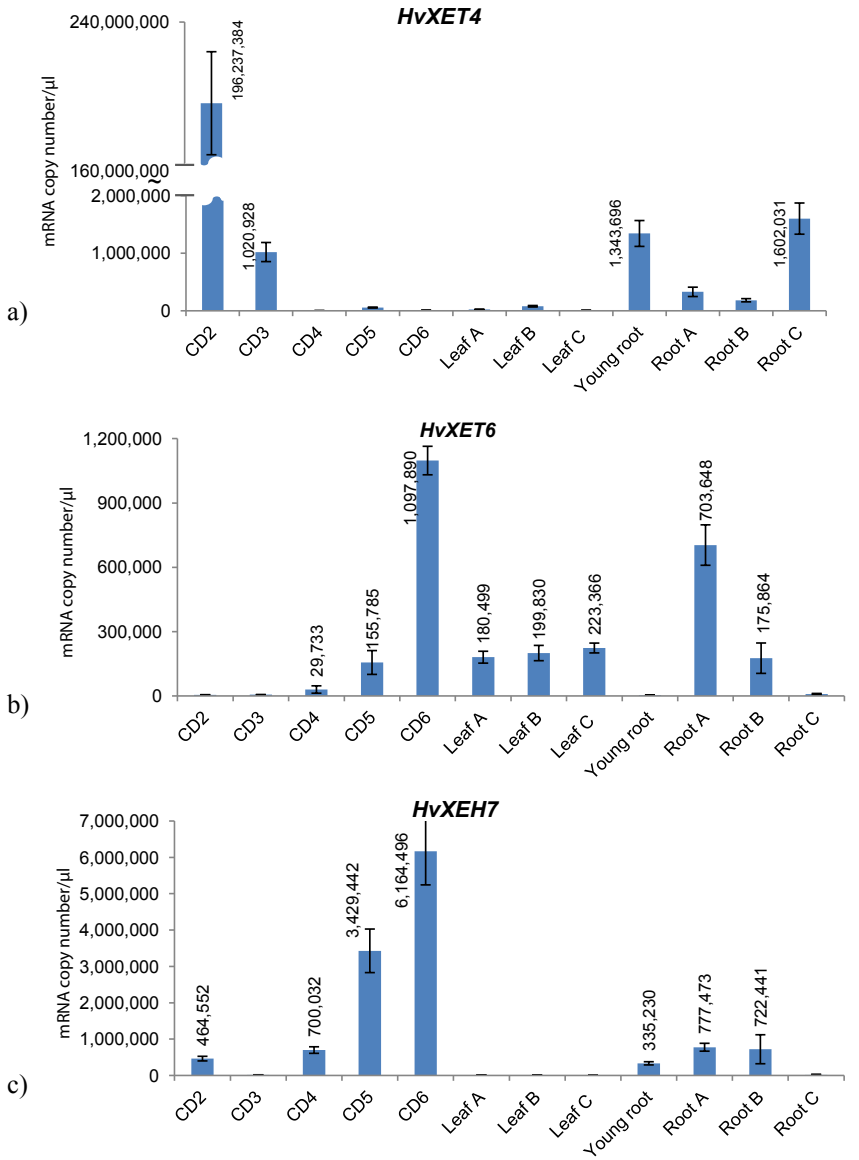

Figure 3. Expression levels of selected *HvXTH* genes. Expression values are given as mRNA copy number/µL with error bars throughout all tissues studied. A. Expression levels of *HvXET4* across all tissues. Note the change in scale on the left so as to better show both the extreme and high expressing values. B. Expression levels of *HvXET6*. C. Expression levels of putative XEH (hydrolase) *HvXEH7*. D. Expression levels of putative EG16 member *HvEG16*. Error bars indicate standard deviation across replicates.

log2(FPKM+) were low in all RNA-seq examined tissues, it was decided to exclude the RT-qPCR data for *HvXET14* from the final results.

3.3 NGS/RNA-seq analysis of barley *XTH* expression levels

RNA-seq experiment results covered 16 tissues from various ages of barley cultivar Morex plants. We obtained chromosomal gene locations and used this information to return FPKM values for the 42 barley *XTH* genes, including the duplicate gene locations for *HvXET8b* and *HvXET14b*, as well as the control genes tubulin and actin that were used as reference genes for RT-qPCR (Supplementary Tables S3 and S4). The most active tissue w.r.t. the RT-qPCR barley *XTH* genes is EMB, which is from 4-day embryos dissected from germinating grains and includes the rapidly expanding coleoptile and roots. It can be expected that these tissues express many *XTH* genes, especially those associated with cell wall expansion. Root tissues in general

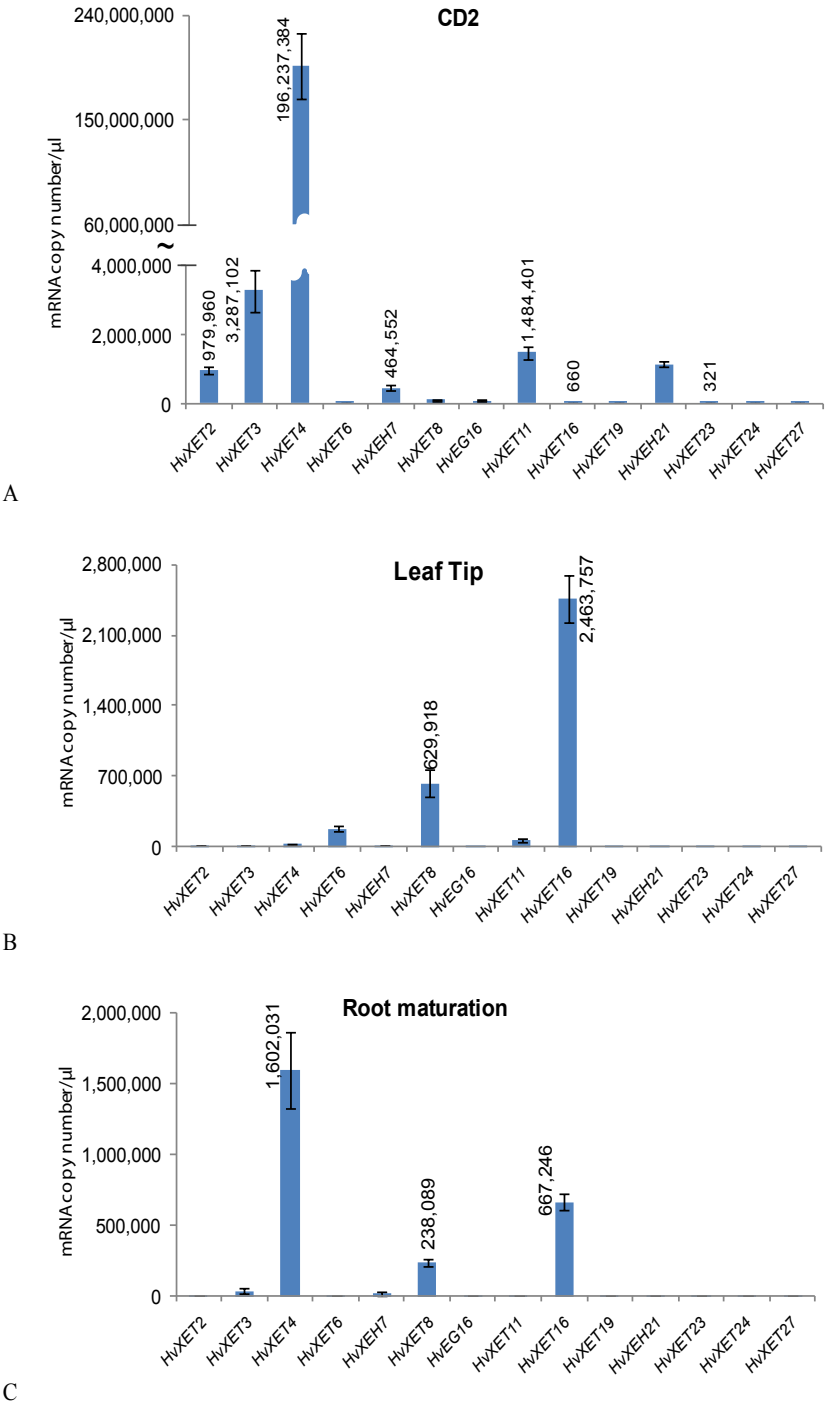

Figure 4. Expression levels of studied *HvXTH* genes in various tissues. Expression values are given as mRNA copy number/µL with error bars. Name of tissues are given as graph titles. Error bars indicate standard deviation across replicates.

have many different *XTH* genes active to the multiple roles required with the dividing, expanding, and maturing cells. The most active gene/s were *HvXET2* and *HvXET3,* which are highly active in most tissues studied. All the other *HvXTH* genes vary widely in their expression patterns with at least one tissue with little to no expression and one or more tissues with high expression values. *HvXET6* is a good example of tissue specificity, with low expression values in most tissues, but a very high 613 FPKM in the NOD internode tissues.

The genes *HvXET27*, *HvXET30*, & *HvXET33* showed no expression in the RNA-seq tissue series. This may be explained by highly specific tissue expression for which the tissue was not represented in these experiments. Indeed, *HvXET27* and *HvXET30* are members of phylogenetic clade IV, which we have recently shown to contain genes that are preferentially or only expressed in floral tissues (Seven et al. 2021), for which there is no barley RNA-seq libraries.

XTH gene expression patterns were compared between the relevant tissues for both the RNA-seq and RT-qPCR data (Table 4). For the EMB tissue comparison, the equivalent-aged root and coleoptile RT-qPCR results were averaged. In addition, the values for the NGS data for *HvXET8* are the sums of their respective *HvXET8a & b* gene values. There is generally good agreement in the levels between the two types of expression data. In particular, *HvXET2* and *HvXET3* are the highest, or close to, in most cases. The expression values co-vary for *HvXEH7*, which is the potential hydrolase gene, with moderately low expression in all three tissues. Variation may also be expected since the RNA-seq data come from the six-row barley cultivar Morex, whereas our RT-qPCR data are for tissues from the Turkish two-row barley cultivar Zeynelağa.

4. Discussion

Bioinformatic analyses of barley EST and genome databases for XTH coding regions revealed the presence of at least 42 putative *HvXTH* sequences. Given that the current version of the barley genome, IBSC v2 of *Hordeum vulgare* cv. Morex, is about 95% complete, it is possible that more *HvXTH* genes are yet to be discovered. Of the 42 putative HvXTH sequences identified here, all were distinguishable by having the highly conserved DEIDFEFLG motif that acts as the enzyme active site (Rose et al. 2002). To our knowledge, this is the largest published number of predicted *XTH* genes for a monocot genome, although it might be expected that wheat, with its hexaploid genome, may have more (Liu et al. 2007). Having large multigene *XTH* families is also seen in other plants; Arabidopsis has 33, Poplar 41 (Geisler-Lee et al. 2006), Grape 37, Sorgum 34 (Eklöf and Brummer, 2010), and *Oryza sativa* is reported as having 29 *XTH* family members (Yokoyama et al. 2004).

XTH enzymes align closely with each other and form a phylogenetic tree that is comprised of six distinguishable groups: Group I, Group II, Group IIIA, Group IIIB, Group IV, and the XTH-precursor EG16 endoglucanase group (Seven et al. 2021). The phylogenetic groups differ from each other not only by their amino acid sequence similarities but also by their enzymatic activities and substrate preferences. Group I and Group II enzymes have XET activity as detectable dominant activity, whereas Group IIIA members show predominantly XEH activity (Rose et al. 2002; Kaewthai et al. 2013). The EG16 group has been shown to contain broad-specificity endoglucanases and likely represents an evolutionary step between progenitor bacterial endohydrolase genes and the rest of the *XTH* gene family (Eklöf et al. 2013).

Table 4 Comparison of barley *XTH* RT-qPCR copies/ul values with FPKM values from relevant RNA-seq experiments. EMB-RT-qPCR is an average of RT-qPCR data for young root and coleoptile. *HvXET8* values for the NGS data are the sum of the *HvXET8a* & *b* gene values.

	'EMB'-RT-qPCR	EMB-NGS	Leaf RT-qPCR	LEAf NGS	Root RT-qPCR	ROOt-NGS
HvXET2	58993	135	5265	51	15857	30
HvXET3	94663	25	6419	117	55959	7
HvXET4	195204	103	6789	59	54386	23
HvXET6	770	36	29283	50	82605	13
HvXEH7	23096	22	1698	16	253580	34
HvXET8	7502	6	25843	11	48962	12
HvEG16	508	7	187	1	8372	3
HvXET11	8131	5	25505	22	13528	2
HvXET16	1910	2	70582	59	26435	40
HvXET19	813	34	16	8	11871	12
HvXEH21	1450	16	27	5	4051	13
HvXET23	1306	6	62	0	2500	3
HvXET24	1938	11	379	0	67847	1
HvXET27	20	0	77	0	1925	0

Such a large number of often highly similar enzymes makes purification of individual isoforms all impossible, and heterologous expression studies of large but numbers of genes are very time-consuming and difficult. Therefore, transcript studies such as RNA-seq and RT-qPCR are better candidates to at least provide knowledge of spatial and temporal expression patterns.

Screening of the translated protein sequences for localisation tags indicated that all sequences except HvEG16 are likely to be targeted to the cell wall. HvEG16 is the barley homologue of PtEG16, a broad specificity glucanase from poplar (Eklöf et al. 2013). It was noted that all members of this clade lack detectable localisation signals.

Despite phylogenetic grouping and differences in potential catalytic activity, all barley XTH and EG16 sequences analysed here share the conserved active site (Figure 2). Additionally, all sequences except HvEG16 share another conserved region of WAT (Figure 2, Table 2) which, when compared to the crystal structure of the poplar PttXET16 (W174), is near the conserved active site, and this tryptophan is likely to be involved in substrate binding at the -2 subsite (Johansson et al. 2004). The residues are replaced by a VDEG sequence in HvEG16, and a similar motif ($^{V}/_{I}X^{D}/_{E}G$) can be seen in EG16 sequences of other species (data not shown). This difference may, therefore, be involved in the catalytic difference between HvEG16 as an EG16 member and the barley XTH enzymes. In addition, HvEG16 lacks the typical C-terminal extension seen in other XTHs that possess 1-4 cysteine residues that are likely to create disulfide bonds to stabilize the protein structure (Eklöf et al. 2013). Thus, the combination of the reduced likelihood of disulphide linkages and the lack of N-glycosylation would suggest that HvEG16 is less stable than the XTH enzymes.

HvEG16 and other monocot EG16 members do have a longer C-terminal region, not seen in dicot EG16s. The role of these extensions and the reason they contain multiple negatively charged amino acid residues remains unknown (Figure 2). Interestingly, HvEG16 and other EG16 enzymes lack the short loop 2 insertion seen in the Group IIIA sequences (Baumann et al. 2007), which is thought to be responsible for the XEH ability of these enzymes, and the lack of this insertion may affect substrate specificity and binding of the EG16 members.

If HvEG16 is indeed a broad specificity endoglucanase such as PtEG16, its role must be different to that of the XEH enzyme HvXEH7, which shows very high expression levels late in the coleoptile time course. However, the *HvEG16* expression pattern is very similar to that of *HvXET21*, which is also a member of Group IIIA and is therefore probably an XEH enzyme. Expression levels of *HvEG16* were very low in most tissues except for moderate levels in root tissues and a peak in CD2, while *HvXET21* has almost identical expression levels except for in CD2 where it is 10 times higher (Table 3). These expression patterns may be interpreted as having a role in cell division, which is occurring in CD2 and in root tips, in root tip border cell dehiscence, and possibly in root hair formation, which occurs near the tip (Root A) and in the elongation zone (Root B).

HvXEH7 mRNA levels were also moderately high in young roots, root tips, and root elongation zone more than 10 times greater than *HvEG16* & *HvXET21*. However, the greatest difference is in its expression in coleoptile tissues where it peaks at over 6 million copies/µL. It seems probable that the role of an XEH enzyme late in the coleoptiles time course is to be involved in recycling of cell wall material for the growing leaf and possibly roots. In the time course of Gibeaut and colleagues (2005), it is not until after day 6 that xyloglucan levels drop, and, even then, it is not by a lot. However, the level of mixed-link glucan (MLG) drops dramatically after day 5, so it is at least possible that HvXEH7 plays some role in MLG degradation and recycling.

Cell wall composition changes between different cell types within a plant during growth of the cell (Trethewey and Harris, 2002). As reported earlier in a detailed study of polysaccharide contents of barley coleoptile cell walls, xyloglucan ratio was observed as relatively constant between day 0 and day 8, but with changes in xyloglucan fine structure and acetylation ratio (Gibeaut et al. 2005). However, *XTH* gene expression levels varied in coleoptiles for many genes in this study (Figure 5), in ways that cannot be accounted for by simply a role in cell expansion, at least not in terms of xyloglucan transferase activity alone. It seems possible, if not highly likely, that at least some of these XTH enzymes are involved in endotransglycosylase activity with other polysaccharides, the potential of which has been demonstrated with barley enzymes previously (Hrmova et al. 2007; Strailova et al. 2020). Increases in *HvXET2, HvXET3*, *HvXET6,* and *HvXEH7* mRNA copy numbers mimic the increase in mixed-linked glucan ratio in coleoptiles in days 2-5, thus enzymes HvXET2, HvXET3, HvXET6 and HvXEH7 might be able to integrate and/or modify MLG within the cell wall. Recent findings of Stratilova et al. (2020) strengthens this hypothesis from another point of view: HvXET3 and HvXET4 were found to be linked with high heterotransglycosylation activities, although, HvXET6 was found to be linked with low heterotransglycosylation activities.

The presence of XET enzymes in developing vascular tissues such as xylem and phloem fibers have been previously reported (Bourquin et al. 2002). Transcript levels of a poplar *XTH* were found to be high during secondary cell wall formation, yet this poplar XTH is a member of Group IIIA XTHs and can predominantly

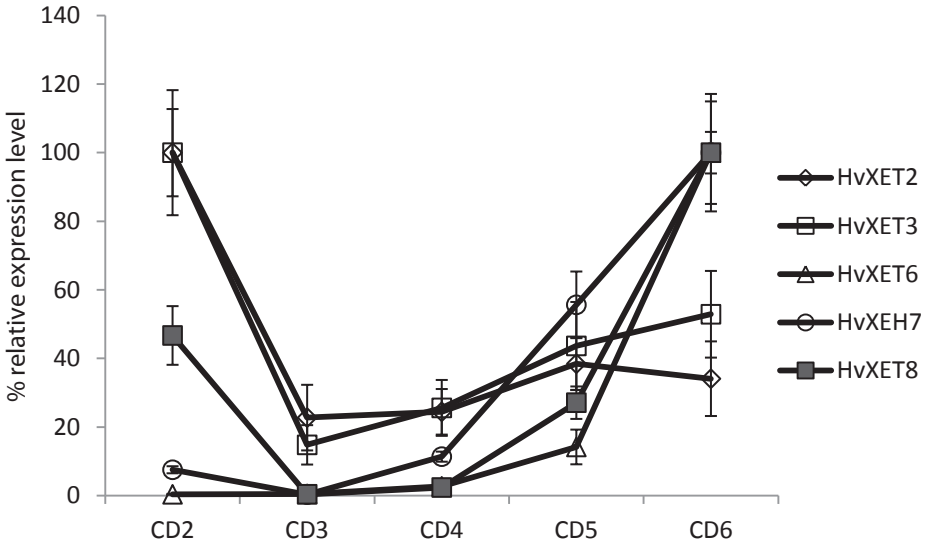

Figure 5. Relative change of expression of *HvXET2, HvXET3, HvXET6, HvXEH7, HvXET8* genes during coleoptile development. Error bars of expression levels are indicated on graph. Error bars indicate standard deviation across replicates.

show XEH activity instead of XET activity (Aspeborg et al. 2005). Expression levels of *HvXET6* and *HvXET8* genes, which are Group II and Group IIIB members respectively, increase during the fifth and sixth day of coleoptile development. Since coleoptile elongation ceases after day 5, the increase in mRNA levels of *HvXET6* and *HvXET8* genes may suggest a role of both gene products in secondary cell wall formation and modification (Gibeaut et al. 2005). An increase in the mRNA copy number of *HvXET8* in leaf tips also contributes to the idea of HvXET8 enzyme having a role in secondary cell wall metabolism.

High expression levels may be necessary when rapid cell expansion is required since for large movement to occur large amounts of polysaccharides need to be cut at around the same time. High amounts of enzymes are likely required for such synchronous action. *HvXET3, HvXET4, HvXET11* and *HvXET21* genes showed examples of the highest expression observed in the study in CD2 samples. CD2 is an early stage of coleoptile growth and is a good example of fast growth, since coleoptile length is increasing more than 100% per day. At this early stage, some cell division is still occurring, which may require a XEH such as HvXET21. The relatively high expression of over 1 million copies/µL of *HvXEH21* indicates an important contribution of an XEH during early development of coleoptile. However, this expression level is much lower than that of *HvXET4,* which has a maximum normalized level of ~196 million copies/µL in CD2 tissues. For comparison, the highest expression level of a cellulose synthase gene in barley cell walls is HvCesA1 with ~1.8 million copies/µL in CD3 tissue (Burton et al. 2004). Such high levels of expression must indicate an important role of HvXET4 in early developing tissue, possibly as a cross-linker between various structural polysaccharides, including cellulose, when their molar ratios are increasing (Gibeaut et al. 2005). An important role of HvXET4 was also proposed by Stratilova et al. (2020) in older tissues such as spike and anther for heterotransglycosylation with proposed pectic oligosaccharides. HvXET3, 4, & 6 have been heterologously expressed, and their enzyme kinetics were studied (Vaaje-Kolstad et al. 2010). Also, high expression of HvXET3 is shown by Stratilova et al. (2020) in young leaf. HvXET6 exhibits higher affinity for xyloglucan as the substrate and also a greater catalytic rate, being approximately 10-fold more efficient than HvXET4 and 20-fold more than HvXET3. Such enzymatic efficiencies would affect the amount of enzyme required to catalyse a given amount of substrate in a given time.

HvXET16 is a Group II example with high levels of expression only in leaf tip and root base tissues. This may be interpreted as HvXET16 having an important role in mature tissue cell wall modification and arrangement as an XET. Other Group II examples were studied, including *HvXET2* and *HvXET3,* which have higher expression in CD2 tissue. Additional to HvXET4 activity, products of *HvXET2* and *HvXET3* can also have coordinative roles in early stage cell wall development.

HvXET24 and *HvXET27* are the genes with the lowest RT-qPCR expression levels in the study. Both genes showed their highest expression in root tip and root elongation samples among the other tissues studied. This finding may indicate that these gene may play some small but specific role in these tissues, or that their highest expression and, hence, most important role is in tissues that were not

studied here. *HvXET27* is a member of the Group IV clade, which as previously mentioned shows highly tissue specific expression in reproductive tissues (Seven et al., 2021). Two of the Arabidopsis members of Group IV, *AtXTH1* & *3*, show their highest expression in floral tissues (Becnel et al. 2006), suggesting some highly specific role. Some of these Group IV clade members have been shown to have very high levels of heterotransglycosylation ability (Seven et al. 2021), which may indicate that they utilise substrates other than xyloglucan.

Previous studies have shown varying levels of correlation between RT-qPCR and RNA-Seq data, with some studies showing 85% of better consistency (Everaert et al. 2017). We see overall similarity in expression patterns, but in a specific comparison between EMB, LEA, & ROO tissues, approximately half of the genes studied followed the same expression pattern. As stated previously, variation is perhaps expected especially for the EMB tissue, where two RT-qPCR results were combined and averaged. Regardless, this comparison has been successful and is useful as a guide for future studies.

In summary, we have shown that the barley genome contains at least 42 active *XTH* genes. There are XTH representatives in each of the clades of the phylogenetic tree, including the Group IV and XTH-precursor EG16 group. *HvXTH* gene expression levels and tissue-specificity showed wide variations, both using RT-qPCR and RNA-Seq. *HvXET4* is the highest in RT-qPCR, with extremely high copy numbers in CD2 tissues. Expression patterns of potential hydrolase genes, *HvXEH7*, *21*, & *10*, differed and must represent different roles for these enzymes in the various tissues. Expression patterns suggestive of secondary cell wall involvement were detected for *HvXET8 & 16*. It is expected that enzyme substrate specificities and mode/s of actions are likely to be similar within the separate branches of the phylogenetic tree; thus, in lieu of actual enzyme data, gene expression profiles combined with knowledge of the cell wall composition of the different tissues is extremely helpful. Together, this information will be useful to predict roles for the various enzymes and, when coupled with substrate specificities and enzyme kinetic data from future experiments, can greatly increase our understanding of cell wall dynamics in barley plants.

Funding
The study was funded by TUBITAK with grant number #214Z248 (Scientific and Technical Research Council of Turkey).

Contribution of authors
Hülya Akdemir and Merve Seven contributed equally to this work.

Acknowledgements
The plant material was kindly provided by the Field Crops Central Research Institute, Ankara, Turkey. The authors would also like to thank N. Rüyam Fettahoğlu BSc., MBA. for technical support.

References

Aspeborg H, Schrader J, Coutinho PM, Stam M, Kallas A et al. (2005). Carbohydrate-active enzymes involved in the secondary cell wall biogenesis in hybrid aspen. Plant Physiology 137: 983-997. doi: 10.1104/pp.104.055087

Atkinson RG, Johnston SL, Yauk YK, Sharma NN, Schröder R (2009) Analysis of xyloglucan endotransglucosylase/hydrolase (*XTH*) gene families in kiwifruit and apple. Postharvest Biology and Technology 51: 149–157. doi: 10.1016/j.postharvbio.2008.06.014

Bailey TL (2011) DREME: Motif discovery in transcription factor ChIP-seq data. Bioinformatics 27: 1653-1659. doi: 10.1093/bioinformatics/btr261

Baumann MJ, Eklof JM, Michel G, Kallas AM, Teeri TT et al. (2007) Structural evidence for the evolution of xyloglucanase activity from xyloglucan endo-transglycosylases: biological implications for cell wall metabolism. Plant Cell 19: 1947-1963. doi: 10.1105/tpc.107.051391

Becnel J, Natarajan M, Kipp A, Braam J (2006) Developmental expression patterns of Arabidopsis *XTH* genes reported by transgenes and Genevestigator. Plant Molecular Biology 61: 451-467. doi: 10.1007/s11103-006-0021-z

Bendtsen JD, Nielsen H, von Heijne G, Brunak S (2004) Improved prediction of signal peptides. SignalP 3.0. Journal of Molecular Biology 340: 783–795. doi: 10.1016/j.jmb.2004.05.028

Bourquin V, Nishikubo N, Abe H, Brumer H, Denman S et al. (2002) Xyloglucan endotransglycosylases have a function during the formation of secondary cell walls of vascular tissues. Plant Cell 14: 3073-3088. doi: 10.1105/tpc.007773

Buchanan BB, Gruissem W, Jones RL (2015) Biochemistry and Molecular Biology of Plants. 2nd ed. Chichester, West Sussex, England: Wiley.

Buels R, Yao E, Diesh CM, Hayes RD, Munoz-Torres M et al. (2016) JBrowse: a dynamic web platform for genome visualization and analysis. Genome Biology 17: 66. doi: 10.1186/s13059-016-0924-1

Burstin J (2000) Differential expression of two barley XET-related genes during coleoptile growth. Journal of Experimental Botany 51: 847-852. doi: 10.1093/jxb/51.346.847

Burton RA, Shirley NJ, King BJ, Harvey AJ, Fincher GB (2004) The CesA gene family of barley. Quantitative analysis of transcripts reveals two groups of co-expressed genes. Plant Physiology 134:24-236. doi: 10.1104/pp.103.032904

Campbell P, Braam J (1998) Co- and/or post-translational modifications are critical for TCH4 XET activity. The Plant Journal 15: 553-561. doi: 10.1046/j.1365-313x.1998.00239.x.

Campbell P, Braam J (1999) Xyloglucan endotransglycosylases: diversity of genes, enzymes and potential wall-modifying functions. Trends in Plant Science. 4: 361–366. doi: 10.1016/s1360-1385(99)01468-5

Carpita N, Tierney M, Campbell M (2001) Molecular biology of the plant cell wall: searching for the genes that define structure, architecture and dynamics. Plant Molecular Biology 47:1-5. doi: 10.1007/978-94-010-0668-2_1

Colmsee C, Beier S, Himmelbach A, Schmutzer T, Stein N et al. (2015) BARLEX - the Barley Draft Genome Explorer. Molecular Plant 8: 964-966. doi: 10.1016/j.molp.2015.03.009

Dash S, Van Hemert J, Hong L, Wise RP, Dickerson JA (2012) PLEXdb: gene expression resources for plants and plant pathogens. Nucleic Acids Research 40: D1194-D1201. doi: 10.1093/nar/gkr938

Deng W, Nickle DC, Learn GH, Maust B, Mullins JI (2007) ViroBLAST: a stand-alone BLAST web server for flexible queries of multiple databases and user's datasets. Bioinformatics 23: 2334-2336. doi: 10.1093/bioinformatics/btm331

Eklöf JM, Brumer H (2010). The *XTH* Gene Family: An update on enzyme structure, function, and phylogeny in xyloglucan remodeling. Plant Physiology 153(2): 456–466. doi: 10.1104/pp.110.156844

Everaert C, Luypaert M, Maag JLV, Cheng QX, Dinger ME et al. (2017) Benchmarking of RNA-sequencing analysis workflows using whole-transcriptome RT-RT-qPCR expression data. Scientific Reports 7: 1559. doi: 10.1038/s41598-017-01617-3

Fry SC, Smith RC, Renwick KF, Martin DJ, Hodge SK et al. (1992) Xyloglucan endotransglycosylase, a new wall-loosening enzyme activity from plants. Biochemical Journal 282: 821-828. doi: 10.1042/bj2820821

Fu MM, Liu C, Wu F (2019) Genome-wide identification, characterization and expression analysis of xyloglucan endotransglucosylase/hydrolase genes family in barley *(Hordeum vulgare*). Molecules 24: 1935. doi:10.3390/molecules24101935

Geisler-Lee J, Geisler M, Coutinho PM, Segerman B, Nishikubo N et al. (2006) Poplar carbohydrate-active enzymes. Gene identification and expression analyses. Plant Physiology 140: 946-962. doi: 10.1104/pp.105.072652

Gibeaut DM, Pauly M, Bacic A, Fincher GB (2005) Changes in cell wall polysaccharides in developing barley (*Hordeum vulgare*) coleoptiles. Planta 221: 729-738. doi: 10.1007/s00425-005-1481-0

Green PB (1980) Organogenesis - a biophysical view. Annual Review of Plant Physiology 31: 51-82. doi: 10.1146/annurev.pp.31.060180.000411

Harvey AJ, Kaewthai N, Hrmova M, Brumer H, Ezcurra I et al (2010) Heterologous expression of diverse barley *XTH* genes in the yeast *Pichia pastoris.* Plant Biotechnology 27: 251–258. doi: 10.5511/plantbiotechnology.27.251

Hématy K, Höfte H (2007) Cellulose and cell elongation. In: Verbelen JP, Vissenberg K (editors). The expanding cell. Berlin, Heidelberg: Springer Berlin Heidelberg, pp. 33-56.

Hoffman M, Jia Z, Pena MJ, Cash M, Harper A et al (2005) Structural analysis of xyloglucans in the primary cell walls of plants in the subclass Asteridae. Carbohydrate Research 340: 1826-1840. doi: 10.1016/j.carres.2005.04.016

Huson DH, Scornavacca C (2012) Dendroscope 3: An interactive tool for rooted phylogenetic trees and networks. Systematic Biology 61: 1061-1067. doi: 10.1093/sysbio/sys062

Hrmova M, Farkas V, Lahnstein J, Fincher GB (2007) A barley xyloglucan xyloglucosyl transferase covalently links xyloglucan, cellulosic substrates, and (1,3;1,4)-beta-D-glucans. Journal of Biological Chemistry 282: 12951-12962. doi: 10.1074/jbc.M611487200

Hrmova M, Farkas V, Harvey AJ, Lahnstein J, Wischmann B et al (2009) Substrate specificity and catalytic mechanism of a xyloglucan xyloglucosyl transferase HvXET6 from barley (*Hordeum vulgare* L.). FEBS Journal, 276(2), 437–456. doi: 10.1111/j.1742-4658.2008.06791.x

Jain M, Nijhawan A, Arora R, Agarwal P, Ray S et al (2007) F-Box proteins in rice. Genome-wide analysis, classification, temporal and spatial gene expression during panicle and seed development, and regulation by light and abiotic stress. Plant Physiology 143 :1467-1483. doi: 10.1104/pp.106.091900

Johansson P, Brumer H, Baumann MJ, Kallas AM, Henriksson H et al (2004) Crystal structures of a poplar xyloglucan endotransglycosylase reveal details of transglycosylation acceptor binding. Plant Cell 16: 874-886. doi: 10.1105/tpc.020065

Kaewthai N, Gendre D, Eklof JM, Ibatullin FM, Ezcurra I et al (2013) Group III-A *XTH* genes of Arabidopsis encode predominant xyloglucan endohydrolases that are dispensable for normal growth. Plant Physiology 161: 440-454. doi: 10.1104/pp.112.207308

Kim D, Langmead B, Salzberg SL (2015) HISAT: a fast spliced aligner with low memory requirements. Nature Methods 12 (4):357-60. doi: 10.1038/nmeth.3317

Langmead B, Salzberg S (2012) Fast gapped-read alignment with Bowtie 2. Nature Methods, 9: 357-359. doi: 10.1038/nmeth.1923

Larkin MA, Blackshields G, Brown NP, Chenna R, McGettigan PA et al (2007) Clustal W and Clustal X version 2.0. Bioinformatics 23: 2947-2948. doi: 10.1093/bioinformatics/btm404

Li H, Handsaker B, Wysoker A, Fennell T, Ruan J et al (2009) The sequence alignment/map (SAM) format and SAMtools. Bioinformatics 25: 2078-2079. doi: 10.1093/bioinformatics/btp352

Li H (2011) A statistical framework for SNP calling, mutation discovery, association mapping and population genetical parameter estimation from sequencing data. Bioinformatics 27 (21): 2987-2993. doi: 10.1093/bioinformatics/btr509

Liu Y, Liu D, Zhang H, Gao H, Guo X et al (2007) The alpha- and beta- expansin and xyloglucan endotransglucosylase/hydrolase gene families of wheat: Molecular cloning, gene expression, and EST data mining. Genomics, 90: 516-529. doi: 10.1016/j.ygeno.2007.06.012

Lombard V, Golaconda Ramulu H, Drula E, Coutinho PM, Henrissat B (2014) The carbohydrate-active enzymes database (CAZy) in 2013. Nucleic Acids Res 42: D490–D495. doi: 10.1093/nar/gkt1178

Maier T, Guell M, Serrano L (2009) Correlation of mRNA and protein in complex biological samples. FEBS Letters 583: 3966-3973. doi: 10.1016/j.febslet.2009.10.036

Maris A, Kaewthai N, Eklof JM, Miller JG, Brumer H et al (2011) Differences in enzymic properties of five recombinant xyloglucan endotransglucosylase/hydrolase (XTH) proteins of *Arabidopsis thaliana*. Journal of Experimental Botany 62: 261-271. doi: 10.1093/jxb/erq263

Mark P, Baumann MJ, Eklof JM, Gullfot F, Michel G et al (2009) Analysis of nasturtium TmNXG1 complexes by crystallography and molecular dynamics provides detailed insight into substrate recognition by family GH16 xyloglucan endo-transglycosylases and endo-hydrolases. Proteins: Structure, Function, and Bioinformatics 75: 820–836. doi: 10.1002/prot.22291

Mbeguie AMD, Hubert O, Baurens FC, Matsumoto T, Chillet M (2009) Expression patterns of cell wall-modifying genes from banana during fruit ripening and in relationship with finger drop. Journal of Experimental Botany 60: 2021-2034. doi: 10.1093/jxb/erp079

Mccann MC, Wells B, Roberts K (1990) Direct visualization of cross-links in the primary plant cell wall. Journal of Cell Science 96: 323-334. doi: 10.1242/jcs.96.2.323

Newton AC, Flavell AJ, George TS, Leat PT, Mullholland B et al (2011) Crops that feed the world 4. Barley: a resilient crop? Strengths and weaknesses in the context of food security. Food Security 3:141. doi: 10.1007/s12571-011-0126-3

Obel N, Neumetzler L, Pauly M (2007) Hemicelluloses and cell expansion. In: Verbelen JP, Vissenberg K (editors). The expanding cell. Berlin, Heidelberg: Springer Berlin Heidelberg, pp. 57-88.

Ouyang S, Zhu W, Hamilton J, Lin H, Campbell M et al (2007) The TIGR rice genome annotation resource: improvements and new features. Nucleic Acids Res 35: D883-887. doi: 10.1093/nar/gkl976

Pertea M, Kim D, Pertea GM, Leek JT, Salzberg SL (2016). Transcript-level expression analysis of RNA-seq experiments with HISAT, StringTie and Ballgown. Nature protocols 11 (9): 1650-1667. doi:10.1038/nprot.2016.095

Rose JK, Braam J, Fry SC, Nishitani K (2002) The XTH family of enzymes involved in xyloglucan endotransglucosylation and endohydrolysis: current perspectives and a new unifying nomenclature. Plant Cell Physiology 43:1421-1435. doi: 10.1093/pcp/pcf171

Sakurai N, Masuda Y (1978) Auxin-induced changes in barley coleoptile cell wall composition. Plant and Cell Physiology 19:1217-1223. doi: 10.1093/oxfordjournals.pcp.a075702

Schünmann PHD, Smith RC, Lång V, Matthews PR, Chandler PM (1997) Expression of *XET*-related genes and its relation to elongation in leaves of barley (*Hordeum* vulgare L.). Plant, Cell & Environment 20: 1439-1450. doi: 10.1046/j.1365-3040.1997.d01-49.x

Seven M, Derman C, Harvey A (2021) Enzymatic characterization of ancestral/group-IV clade xyloglucan endotransglycosylase/hydrolase enzymes reveals broad substrate specificities. The Plant Journal 106: 1660–1673. doi: 10.1111/tpj.15262

Smith RC, Matthews PR, Schünmnn PHD, Chandler PM (1996) The regulation of leaf elongation and xyloglucan endotransglycosylase by gibberellin in 'Himalaya' barley (*Hordeum vulgare* L.). Journal of Experimental Botany 47: 1395-1404. doi: 10.1093/jxb/47.9.1395

Stratilova B, Sestak S, Mravec J, Garajova S, Pakanova Z et al (2020) Another building block in the plant cell wall: barley xyloglucan xyloglucosyl transferases link covalently xyloglucan and anionic oligosaccharides derived from pectin. The Plant Journal 104: 752–767. doi: 10.1111/tpj.14964

Strohmeier M, Hrmova M, Fischer M, Harvey AJ, Fincher GB et al (2004) Molecular modeling of family GH16 glycoside hydrolases: potential roles for xyloglucan transglucosylases/hydrolases in cell wall modification in the poaceae. Protein Science 13: 3200-3213. doi: 10.1110/ps.04828404

Trapnell C, Williams BA, Pertea G, Mortazavi A, Kwan G et al (2010). Transcript assembly and quantification by RNA-Seq reveals unannotated transcripts and isoform switching during cell differentiation. Nature Biotechnology 28 (5): 511-515. doi: 10.1038/nbt.1621

Trethewey JAK, Harris PJ (2002) Location of (1 → 3)- and (1 → 3), (1 → 4)-β-D-glucans in vegetative cell walls of barley (*Hordeum vulgare*) using immunogold labelling. New Phytologist 154: 347-358. doi: 10.1046/j.1469-8137.2002.00383.x

Vaaje-Kolstad G, Farkaš V, Hrmova M, Fincher GB (2010) Xyloglucan xyloglucosyl transferases from barley (*Hordeum vulgare* L.) bind oligomeric and polymeric xyloglucan molecules in their acceptor binding sites. Biochimica et Biophysica Acta - General Subjects 1800: 674–684. doi: 10.1016/j.bbagen.2010.04.001

Vorwerk S, Somerville S, Somerville C (2004) The role of plant cell wall polysaccharide composition in disease resistance. Trends Plant Science 9: 203-209. doi: 10.1016/j.tplants.2004.02.005

Yokoyama R, Nishitani K (2001) A comprehensive expression analysis of all members of a gene family encoding cell-wall enzymes allowed us to predict cis-regulatory regions involved in cell-wall construction in specific organs of Arabidopsis. Plant & Cell Physiology 42: 1025–1033. doi: 10.1093/pcp/pce154

Yokoyama R, Rose JK, Nishitani K (2004) A surprising diversity and abundance of xyloglucan endotransglucosylase/hydrolases in rice. Classification and expression analysis. Plant Physiology 134: 1088-1099. doi: 10.1104/pp.103.035261

Zhang MP, Liu Y-H, Chang C-S, Zhi H, Wang S et al (2018) Quantification of gene expression while taking into account RNA alternative splicing. Genomics. 111 (6): 1517-1528. doi: 10.1016/j.ygeno.2018.10.009

Zykwinska A, Thibault J-F, Ralet M-C (2008) Competitive binding of pectin and xyloglucan with primary cell wall cellulose. Carbohydrate Polymers 74: 957-961. doi: 10.1016/j.carbpol.2008.05.004